Vaginal Submucosal Dendritic Cells, but Not Langerhans Cells, Induce Protective Th1 Responses to Herpes Simplex Virus–2

Xinyan Zhao,[1] Eszter Deak,[1] Kelly Soderberg,[1] Melissa Linehan,[1] David Spezzano,[2] Jia Zhu,[2] David M. Knipe,[2] and Akiko Iwasaki[1]

[1]*Department of Epidemiology and Public Health, Yale University School of Medicine, New Haven, CT 06520*
[2]*Department of Microbiology and Molecular Genetics, Harvard Medical School, Boston, MA 02115*

Abstract

Herpes simplex virus (HSV) type 2 infection occurs primarily at the genital mucosal surfaces and is a leading cause of ulcerative lesions. Despite the availability of animal models for HSV-2 infection, little is known regarding the mechanism of immune induction within the vaginal mucosa. Here, we examined the cell types responsible for the initiation of protective Th1 immunity to HSV-2. Intravaginal inoculation of HSV-2 led to a rapid recruitment of submucosal dendritic cells (DCs) to the infected epithelium. Subsequently, CD11c$^+$ DCs harboring viral peptides in the context of MHC class II molecules emerged in the draining lymph nodes and were found to be responsible for the stimulation of IFNγ secretion from HSV-specific CD4$^+$ T cells. Other antigen-presenting cells including B cells and macrophages did not present viral peptides to T cells in the draining lymph nodes. Next, we assessed the relative contribution to immune generation by the Langerhans cells in the vaginal epithelium, the submucosal CD11b$^+$ DCs, and the CD8α^+ lymph node DCs. Analysis of these DC populations from the draining lymph nodes revealed that only the CD11b$^+$ submucosal DCs, but not Langerhans cell–derived or CD8α^+ DCs, presented viral antigens to CD4$^+$ T cells and induced IFNγ secretion. These results demonstrate a previously unanticipated role for submucosal DCs in the generation of protective Th1 immune responses to HSV-2 in the vaginal mucosa, and suggest their importance in immunity to other sexually transmitted diseases.

Key words: genital mucosa • cytokines • lymph node • epithelium • sexually transmitted disease

Introduction

The vaginal mucosa is under constant exposure to infectious agents, and is consequently surveyed by a network of dendritic cells (DCs).* DCs are present in both the stratified squamous epithelial layer as Langerhans cells (LCs) and in the submucosal lamina propria in the vagina. Although a similar population of the latter found in the skin, known as the dermal DCs, has been shown to possess similar immunostimulatory capacity to epidermal LCs in vitro (1, 2), virtually nothing is known about the role of submucosal vaginal DCs in the induction of mucosal immunity. Unlike other mucosal tissues, the female reproductive tract undergoes dramatic hormone-dependent changes over the course of the menstrual cycle. Previous studies have shown that mice are susceptible to intravaginal (ivag) herpes simplex virus (HSV) type 2 infection only during the catabolic metestrous-2 and the diestrous phases of the estrous cycle (3–6). Thus, treatment of mice with progesterone (Depo-Provera®), which maintains the mice at the diestrous-like stage, is often required for consistent ivag infection with HSV-2. However, the precise mechanism by which the progesterone treatment increases the susceptibility to ivag HSV-2 infection is unknown. One potential mechanism relates to the thickness of the vaginal epithelial layer. With the increase in serum estrogen levels, the epithelial cell layer thickens during the estrous stage. Subsequently, with the increase in the progesterone levels and decrease in the estrogen, the superficial layers of the vaginal epithelium are delaminated during metestrous phases and become maximally thin by the diestrous stage. Another possible mechanism for the increased susceptibility to HSV-2 ivag infection in progesterone-dominant mice is the lack of antigen-presenting cells (APCs) at the sites of infection re-

Address correspondence to Akiko Iwasaki, Dept. of Epidemiology and Public Health, 60 College St., LEPH 716, New Haven, CT 06520. Phone: 203-785-2919; Fax: 203-785-7552; E-mail: akiko.iwasaki@yale.edu

*Abbreviations used in this paper: a.i., after infection; APC, antigen-presenting cell; DC, dendritic cell; HSV, herpes simplex virus; ivag, intravaginal(ly); LC, Langerhans cell; TK, thymidine kinase.

quired to initiate immune responses, as frequency of LCs may differ at each stage of the menstrual cycle within the mouse vagina. Thus, it is important to determine the distribution and function of DCs during the estrous cycle, as it relates to the susceptibility of the female host to infectious agents such as HSV-2.

A mouse model of ivag infection using HSV-2 thymidine kinase (TK) mutant strain (6, 7) has provided important insights into the mechanism of immune resistance to HSV-2. The TK[−] mutant HSV-2 causes mild vaginal pathologies that resolve within 7 d but do not result in neurologic diseases, making it an ideal virus with which to study immune induction to vaginal HSV-2 infection. Intravaginal infection with TK^{−} HSV-2 is known to induce protective immunity that is primarily mediated by IFNγ secreted from CD4^{+} T cells (8, 9) and HSV-2–specific IgG (10, 11). However, the viral infection events and APC types involved in inducing the T cell responses to HSV-2 are poorly understood. A recent paper has demonstrated that B cells represent the major cell type recruited from the vaginal mucosa to the draining lymph nodes after ivag HSV-2 delivery, suggesting a role for B cells in the immune initiation process (12). In this paper, no migration of LCs from the vagina to the draining lymph nodes was detected, raising the question about whether LCs are involved in antigen presentation and T cell activation in the draining lymph nodes.

To understand the mechanism of immune induction by DCs and other APCs to HSV-2 infection in the vaginal mucosa, we examined the distribution, phenotype, and function of DCs at the sites of infection and in the draining lymph nodes. By following HSV-2 infection and DC distribution by immunofluorescence microscopy, we demonstrate that HSV-2 productively infects the vaginal epithelium exclusively and that submucosal DCs are recruited to the lamina propria bordering the infected epithelium within 24 h after infection (a.i.). In addition, we present the time course of the appearance of DCs harboring HSV-2 peptides in the draining lymph nodes, the induction of HSV-2–specific CD4^{+} T cell responses in the local draining lymph nodes and the subsequent migration of these primed T cells to systemic lymphoid organs. Furthermore, by isolating specifically the LCs and submucosal DCs from the draining lymph nodes, we demonstrate that the primary cells that migrate from the vaginal mucosa and present viral antigens to CD4^{+} T cells are non-LC submucosal DCs. The results from this paper provide the first evidence that DCs are recruited rapidly to the lamina propria bordering the infected vaginal epithelial cells infected with HSV-2, and that these CD11c^{+}/CD11b^{+} submucosal DCs, but not LCs or CD8α^{+} DCs, B cells, or other APCs, phagocytose viral antigens and migrate to local lymph nodes to induce protective Th1 CD4^{+} T cell responses.

Materials and Methods

Virus. HSV-2 strains 186TKΔKpn were constructed as described previously (13) and propagated and assayed on Vero cells (14). All stocks were titered on the Vero cell line before use in the ivag infections.

Animals and HSV-2 Infection. 6–8-wk-old female BALB/c mice were obtained from the National Cancer Institute. Mice transgenic for TCR that recognizes OVA323–339 peptide in the context of I-A[d] (DO11.10TCR-αβ transgenic mice) on a BALB/c background were provided by Dr. Dennis Loh (Washington University, St. Louis, MO). The estrous stage of mice was determined from analysis of vaginal smears taken by a calcium-alginate swab (Fisher Scientific) and stained with Diff-Quik Stain (Dade Behring) according to manufacturer's instruction. Stained cells were carefully examined and the estrous stage of each mouse was identified as diestrous, estrous, metestrous-1, or metestrous-2 according to a previously established protocol (15, 16). For virus infection studies, mice were injected subcutaneously in the neck ruff with Depo-Provera® (Pharmacia & Upjohn Diagnostics) at 2 mg/mouse in 100-μl volume 5–7 d before infection, swabbed with calcium-alginate and inoculated ivag with either 10[7] PFU of HSV-2 strain 186TKΔKpn or inoculated with noninfected Vero cell lysate (mock infection) in 10 μl volumes using a blunt-ended micropipette tip. All procedures used in this paper complied with federal guidelines and institutional policies by the Yale Animal Care and Use Committee.

Antibodies. The following antibodies were used for the identification of cell populations: anti-CD11c (N418), anti-CD11b (M1/70), anti-CD8α (53-6.7), anti-DEC205 (NLDC-145), and anti–MHC class II (M5/114). The aforementioned antibodies were purchased from BD Biosciences, except for NLDC-145 and N418 which were purified from hybridoma supernatants. The LC-specific anti-gp40 antibody G8.8 developed by Andrew Farr (University of Washington, Seattle, WA), was obtained from the Developmental Studies Hybridoma Bank developed under the auspices of the National Institute of Child Health and Human Development and maintained by the University of Iowa Department of Biological Sciences. For localization of HSV-2–infected cells, polyclonal rabbit antiserum against HSV-2 was purchased from BioGenex.

Double Immunofluorescence Staining of Vaginal Tissues. To examine the distribution of DC in relation to HSV-2 infection within the vagina, frozen sections of vagina were stained with a variety of antibodies in a procedure similar to that described previously (17) with minor modifications. In brief, 6–8-μm frozen sections were fixed in acetone and blocked with TNB buffer (3% Casein in PBS; NEN Life Science Products) containing 5% normal donkey serum. To block endogenous biotin, the sections were further treated with the Avidin–Biotin block (Vector Laboratories), and endogenous peroxidase activity was quenched with 1% H₂O₂. The primary antibody was applied at 5 μg/ml for 1.5 h at room temperature. Slides were washed and incubated with biotin-conjugated donkey F(ab′)₂ anti–hamster IgG (Jackson ImmunoResearch Laboratories, Inc.), followed by incubation with streptavidin–HRP conjugate (Zymed Laboratories). The antigens were detected using tyramide-FITC (NEN Life Science Products Inc.) according to the manufacturer's instructions. After the development with the first antibody, sections were blocked with Avidin–Biotin, followed by incubation with 2% H₂O₂. The sections were subsequently stained with the second primary antibody in a similar manner as described above in the previous paragraph with proper species-specific secondary antibody. The slides were developed with tyramide-tetramethylrhodamine (NEN Life Science Products). At the end of the staining, slides were washed and incubated with DAPI (Molecular Probes) and mounted with Fluoromount-G (Southern Biotechnology Associates, Inc.). The stained

slides were analyzed by fluorescence microscopy (Leitz Orthoplan 2) with a 20× objective lens or by confocal microscopy using a confocal laser microscope (model LSM510; Carl Zeiss MicroImaging, Inc.) with a 20 or 40× objective lens with water.

Preparation of Dendritic Cells and Other APCs. DCs and other APCs were prepared from draining lymph nodes of ivag HSV-2–infected mice as described previously (18). In brief, draining lymph nodes (inguinal and iliac), or in some cases spleen and mesenteric lymph nodes, were excised from infected mice at various time points. Lymph nodes were digested with collagenase D and DNase I and incubated in the presence of 5 mM EDTA at 37°C for 5 min. A single-cell suspension was prepared, and cells were incubated with anti–mouse CD11c-coated magnetic beads (Miltenyi Biotech) and selected on MACS separation columns twice. Positively selected cells were routinely 80–90% DC based on CD11c and MHC class II staining by flow cytometry. For CD11c-depleted B cells and MHC class II$^+$ cells, CD11c$^+$ cells were depleted from the draining lymph node suspension by labeling CD11c$^+$ cells with the MACS separation beads (anti-CD11c–coated beads) followed by selection using the LD depletion column (Miltenyi Biotech). B220$^+$ or I-A^{d+} cells were obtained from CD11c-depleted population by staining with FITC-conjugated B220 or FITC-conjugated anti–MHC class II antibody and selected on anti-FITC–conjugated MACS beads according to the manufacturer's instructions (Miltenyi Biotech). The B220$^+$- and I-A^{d+}–selected cells were routinely 80–90% pure as determined by FACS® (see Fig. 4 a). To prepare activated DCs for experiments described in Fig. 3 e, transiently adherent DCs were prepared from splenocytes of BALB/c mice as described previously (19). For FACS® sorting of LCs and submucosal DCs, CD11c-enriched cells from the draining lymph nodes were stained with anti-gp40 (rat IgG2a) followed by FITC-conjugated anti–rat Fab (Jackson ImmunoResearch Laboratories). Cells were washed extensively and stained with anti-CD11b and anti-CD11c. The submucosal DCs (CD11b$^+$/gp40$^-$/CD11c$^+$) and LCs (CD11c$^+$/gp40$^+$) were sorted to 99% purity. In separate experiments, CD8α$^+$ and CD11b$^+$ DCs were isolated from the draining lymph nodes after staining of CD11c-enriched population with antibodies to CD8α, CD11b, and CD11c. The CD8α$^+$ DCs (CD8α$^+$/CD11c$^+$/CD11b$^-$) and CD11b$^+$ DCs (CD11b$^+$/CD11c$^+$/CD8α$^-$) were FACS®-sorted to 99% purity.

Isolation of CD4$^+$ T Cells. Draining lymph nodes (inguinal and iliac) were excised from infected mice at the indicated time points. Single-cell suspensions of lymph node cells were made by dissociating cells through the cell strainer. Cells were washed twice with PBS, stained with FITC-conjugated anti-CD4 antibody (eBioscience), and selected with magnetic beads conjugated to anti-FITC antibody (Miltenyi Biotech) according to the manufacturer's instructions. Selected cells were checked by flow cytometry and were routinely 90–95% pure CD4$^+$ T cells. For experiments involving ovalbumin-specific T cells (Fig. 3 f), in vitro–activated CD4$^+$ T cells were prepared by incubating total splenocytes from DO11.10 mice in the presence of the ovalbumin peptide (OVA323–339) for 72 h. CD4$^+$ T cells were purified using MACS separation as described in the previous paragraph.

Stimulation of HSV-2–specific CD4$^+$ T Cells by DCs and Other APCs. To determine the ability of the DCs to stimulate HSV-2–specific T cells, 10^5 CD4$^+$ T cells from draining lymph nodes of mice infected ivag with 186TKΔKpn 5 d before were co-cultured with 10^5 APCs in the presence of the heat-inactivated virus or heat-inactivated nonvirus-infected cell lysate control. Virus-infected (186TKΔKpn) or uninfected Vero cell control lysate was heat-inactivated at 56°C for 30 min, at which point they were

determined noninfectious as assayed by addition to susceptible Vero cells (unpublished data). No difference in proliferation or cytokine secretion was detected between wells that received heat-inactivated cell lysate and those that received media alone (unpublished data). T cells were stimulated for 72 h in vitro by various APCs and the supernatant was tested for cytokines by ELISA as described previously (18). To determine the source of cytokines in the co-culture, T cells or APCs, in some experiments, were inactivated by irradiation at 3,000 rad.

Detection of Viral DNA in Purified DCs. Total DNA from purified DCs or from infected vaginal epithelium was obtained by resuspending the cell pellet in STE buffer (0.1 M NaCl, 10 mM Tris-Cl, 1 mM EDTA, pH 8.0) and boiling for 10 min. HSV-2 glycoprotein B gene–specific primers HSV2a-1 (forward, 5′ CTGGTCAGCTTTCGGTACGA 3′) and HSV2a-2 (reverse, 5′ CAGGTCGTGCAGCTGGTTGC 3′) were used to amplify viral DNA as described previously (20). The presence of genomic DNA was determined by PCR amplification of housekeeping gene hypoxanthine-guanine phosphoribosyl transferase (HPRT) using primers (forward, 5′CTGGAGGCAGGAAGGAGTCC 3′; reverse, 5′ GGTCCTCCTACGTTGTCTGG 3′) and amplifying for 35 cycles. The lower limit of detection using our PCR protocol was calculated by performing PCR on purified viral DNA as follows. Cell-free 186TKΔKpn HSV-2 virions propagated in Vero cells were collected from the culture supernatant by centrifugation at 20,000 g at 15°C (rotor SW27; Beckman Coulter) for 45 min. The pellet containing cell-free virions was collected, and viral genomic DNA was purified using QIAamp DNA Mini Kit (QIAGEN). Eight 10-fold dilutions of DNA were made, and 1 μl of each dilution was used as a template to amplify viral DNA using the HSV2a-1 and HSV2a-2 primers as described above in the previous paragraph. The lower limit of detection by our PCR protocol was 30 viral particles per reaction. Similarly, by isolating total DNA from in vitro–infected Vero cells, our PCR protocol was able to consistently detect as little as one infected cell per reaction.

Real-time PCR Analysis. TaqMan Real-time PCR amplification and detection were performed using a sequence detector (model ABI 7700; PE Biosystems). HSV-2 TK gene-specific primers (F145, 5′ CTGTTCTTTTATTGCCGTCATCG 3′ and R263, 5′ GTCCATCGCCGAGTACGC 3′) and a fluorescence-labeled probe (5′ Fam-TTTGAACTAAACTCCCCCC-ACCTCGC-Tamra 3′) were used to detect HSV-2 viral DNA. Reactions were performed in 50-μl volumes containing TaqMan Universal PCR Master Mix (PE Biosystems) with a final concentration of 250 nM of each primer and 200 nM of TaqMan probe, and reactions were amplified for 40 cycles. 10^4 cell equivalent amount of DNA samples extracted from draining lymph node DCs were run in parallel with duplicated viral DNA standards to determine the quantity of viral DNA molecules. For viral DNA standards, purified HSV-2 viral DNA was serially diluted in the presence of 30 ng genomic DNA of uninfected CV-1 cells. The viral DNA was diluted such that 1 μl of the sample contained 10^6, 10^5, 10^4, 10^3, 10^2, 10, and 10^0 of HSV-2 DNA. As little as two viral DNA copies could be routinely detected in these assays.
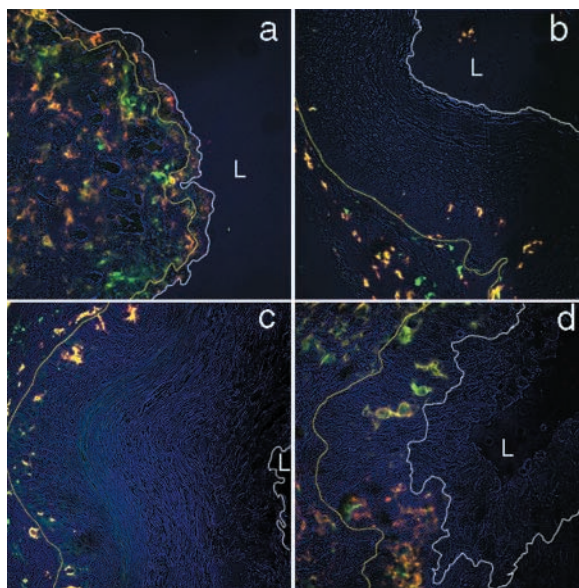
Results

LC and DC Distribution in the Vaginal Mucosa during the Estrous Cycle. To examine the distribution of DCs in the uninfected vaginal epithelium and lamina propria during

the estrous cycle, frozen sections of vagina from mice at different stages of the estrous cycle were doubly stained with antibodies to CD11c and MHC class II and analyzed by confocal microscopy (Fig. 1). The epithelial cell thickness was found to be minimal at diestrous (2–3 cells thick; Fig. 1 a) and maximal at estrous (12 cells thick; Fig. 1 b). During the catabolic metestrous-1 stage, the cornified vaginal epithelium begins to shed (Fig. 1 c), and is replaced by numerous neutrophils in the lumen with a few cell layers of remaining epithelium at the metestrous-2 phase (Fig. 1 d). Interestingly, the LCs (MHC class II$^+$ [red]/CD11c$^+$ [green]; yellow) are distributed abundantly during the diestrous and metestrous-2 stages throughout the epithelial layer, but only sparsely near the base of the epithelium during estrous and metestrous-1 phases. Notably, there are no LCs near the lumen of the vagina at these latter stages. Thus, LCs localize near the lumen of the vagina only during the catabolic phases in which the epithelium is maximally thin.

Submucosal DC Recruitment to the Infected Epithelium. When mice at different stages of the estrous cycle were infected with HSV-2, only those at diestrous and late metestrous-2 phases or those that received Depo-Provera® treatment became infected (unpublished data), which is consistent with previous reports (3–6). In an effort to follow the ivag HSV-2 infection and to understand the mechanism of immune induction to HSV-2, mice pretreated with Depo-Provera® were infected ivag with 10^7 PFU of the TK$^-$ strain of HSV-2 (186TKΔKpn). Frozen sections

of the vagina of mice infected for 24 h, 48 h, or 5 d were doubly labeled with antibodies to HSV-2 (red) and CD11c (green) (Fig. 2). In the mock-infected mice, the epithelium and lamina propria contained abundant CD11c$^+$ cells with a similar frequency to those present in uninfected mice (Fig. 2, a, c, e, and g). However, 24 h after ivag infection with HSV-2, numerous CD11c$^+$ DCs were found in the lamina propria just beneath the infected epithelium, creating multiple foci of submucosal DCs (Fig. 2 b). These submucosal DCs were all CD11b$^+$ as demonstrated for the dermal DCs (21). A detailed analysis of the DCs near the
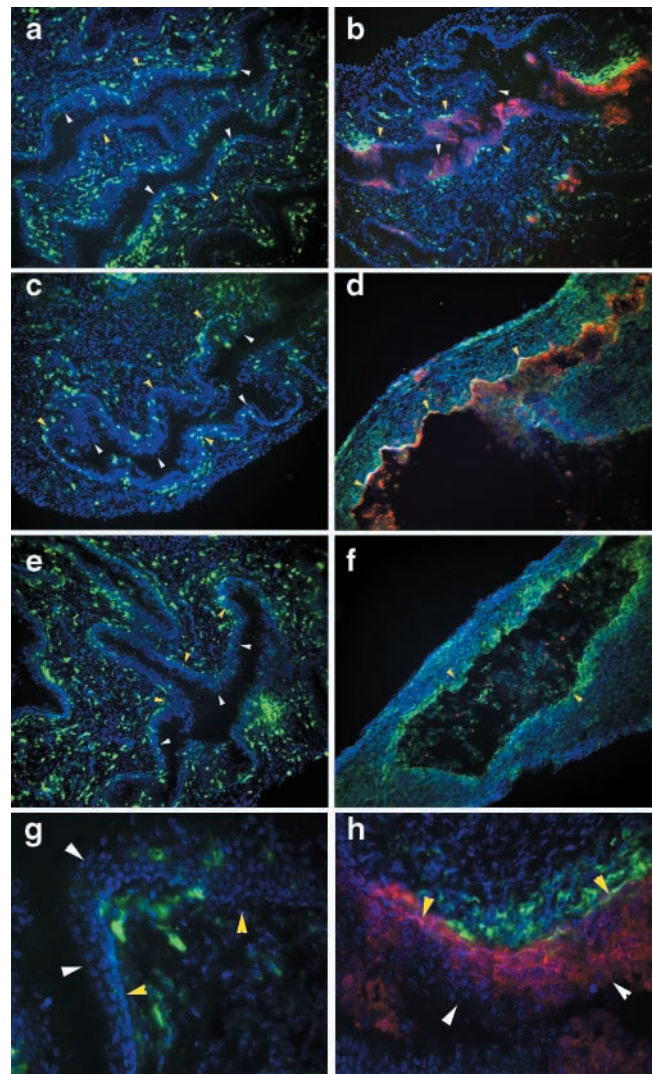

Figure 2. DC recruitment to the HSV-2–infected vaginal epithelium. BALB/c mice pretreated with Depo-Provera® were inoculated with ivag TK mutant HSV-2 (b, d, f, and h), or with control cell lysate (a, c, e, and g), and vaginal tissues were collected for staining with antibodies against CD11c (green) and HSV-2 (red) at 24 h (a, b, g, and h), 48 h (c and d), or 5 d (e and f) a.i. The nucleus was visualized by staining with DAPI (blue). Images were captured using a 20× objective lens (a–f) or with 40x lens (g and h). The epithelial layer is indicated by the white arrowheads (luminal edge) and yellow arrowheads (basement membrane). Panels g and h represent higher magnification images of the selected areas in panels a and b, respectively.

Figure 1. LC distribution in the vaginal epithelium during the estrous cycle. Frozen sections of vaginal tissues from mice at diestrous (a), estrous (b), metestrous-1 (c), and metestrous-2 (d) phases were stained with antibodies against MHC class II (red) or CD11c (green) and analyzed by confocal microscopy. Confocal images are overlaid with light transmission microscopy images to denote tissue morphology. The white line indicates the luminal edge of the epithelium, whereas the yellow line indicates the basement membrane. The images were captured using objective lenses of 20× (a–c) or 40× (d). L, lumen.

infected epithelium showed no evidence of direct infection by HSV-2 (Fig. 2 h). By 48 h, the foci of DCs were replaced by a massive infiltration of DCs throughout the lamina propria and the entire length of the epithelial layer was now infected, which resulted in the shedding of the virally infected, dying epithelia. By day 5, the vaginal tract was devoid of most epithelial cells (Fig. 2 f) and virally infected cells became rare. By days 7–10, the anatomy of the vaginal mucosal returned to normal with the exception of the appearance of clusters of lymphocytes near the lumen (unpublished data). Thus, successful HSV-2 replication occurred exclusively in the epithelial cells in progesterone-dominant mice; CD11c$^+$/CD11b$^+$ submucosal DCs were recruited to the lamina propria just beneath the infected epithelium as early as 24 h a.i.

Dendritic Cells Present HSV-2 Peptides in the Draining Lymph Node. To understand the role of DCs in the immune induction to HSV-2, we collected DCs in the draining lymph nodes at different time points after ivag infection with 186TKΔKpn. The draining lymph node cells were positively selected on the basis of CD11c expression using magnetic beads. The percentage of DCs expressing co-stimulatory molecules CD80 and CD86 increased within the first few days and returned to normal levels by 7 d a.i. (Fig. 3 a). Next, the ability of the draining lymph node DCs to present in vivo–derived viral antigens was examined by co-culture of CD4$^+$ T cells isolated from day 5 draining lymph nodes of HSV-2–infected mice in the absence of exogenously added antigens. The cytokine secretion induced by DCs from HSV-2–specific CD4$^+$ T cells was detected as early as 2 d a.i. and persisted for up to 10 d a.i. (Fig. 3, b–d). Significant levels of IFNγ were induced by DCs draining the lymph nodes between 2 and 5 d a.i. (Fig. 3 b). The same DCs stimulated much lower levels of IL-10 (Fig. 3 c) and barely detectable levels of IL-4 (Fig. 3 d) from CD4$^+$ T cells. None of these cytokines were detected from CD4$^+$ T cells isolated from mock-infected mice stimulated under these conditions (unpublished data). All cytokines (IFNγ, IL-4, and IL-10) were found to be secreted from CD4$^+$ T cells, but not DCs, because cytokine levels diminished in the co-culture of irradiated CD4$^+$ T cells with live DCs, but not in cultures of irradiated DCs with live CD4$^+$ T cells (unpublished data).

Although cytokines were not detected from the CD4$^+$ T cells in noninfected mice stimulated with DCs from infected mice, it was possible that the cytokine secretion observed in the DC–T cell co-culture in Fig. 3 (b–d) reflected nonspecific stimulation of in vivo–primed T cells by the activated DCs in the draining lymph nodes. To address these possibilities, we performed two sets of experiments. First, to determine whether the draining lymph node T cells secreted cytokines in a nonantigen-specific manner, CD4$^+$ T cells from mice infected for 4 d with HSV-2 were co-cultured with in vitro–stimulated transiently adherent splenic DCs. In the absence of viral antigen, even though the transiently adherent overnight-stimulated DCs were fully activated, they were not able to induce secretion of cytokines from the draining lymph node CD4$^+$ T cells
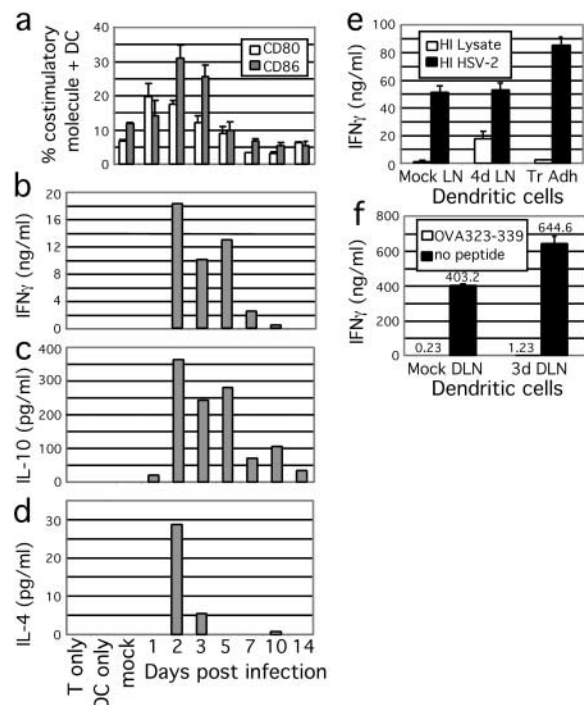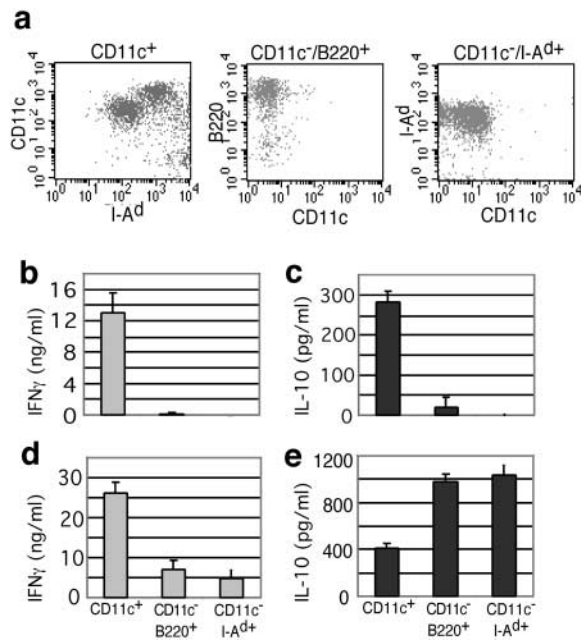

Figure 3. DCs in the draining lymph nodes up-regulate co-stimulatory molecules and present viral antigen. DCs were isolated from the draining lymph nodes of mice inoculated ivag with HSV-2 or with control cell lysate (mock) using magnetic beads. (a) Co-stimulatory molecules CD80 and CD86 expression levels were determined by flow cytometry. (b–d) Cytokine secretion from HSV-2–specific CD4$^+$ T cells co-cultured with draining lymph node DCs, or from CD4$^+$ T cells (day 5 a.i.) or DCs (day 3 a.i.) alone, were analyzed by ELISA. CD4$^+$ HSV-2–specific T cells were obtained from the draining lymph node of day 5 ivag HSV-2–infected mice by positive selection using magnetic selection. To demonstrate the antigen specificity of the T cell responses, (e) DCs isolated from the draining lymph nodes of either mock-infected or day 3 HSV-2–infected mice, or in vitro–activated transiently adherent splenic DCs, were coincubated with day 5 draining lymph node CD4$^+$ T cells in the presence (filled) or absence (white) of exogenously added virus antigens. T cell IFNγ secretion was measured by ELISA. (f) To demonstrate the requirement of specific antigen for T cell activation by the draining lymph node DCs, in vitro–activated OVA-specific T cells were coincubated with DCs isolated from the draining lymph nodes of either mock-infected or day 4 HSV-2–infected mice in the presence (filled) or absence (white) of OVA323–339 peptide. T cell IFNγ secretion was measured by ELISA.

(Fig. 3 e). Thus, the draining lymph node CD4$^+$ T cells require recognition of viral antigens for activation and secretion of cytokines. Second, to determine whether the DCs in the draining lymph nodes stimulated T cells nonspecifically, CD4$^+$ T cells from DO11.10 mice were preactivated in vitro in the presence of OVA323–339 peptide. These maximally activated clonal T cells were coincubated with draining lymph node DCs from day 3 HSV-2–infected mice in the presence or absence of the OVA peptide. Although activated DO11.10 T cells secreted large amounts of cytokines in the presence of the specific peptide, day 3 a.i. draining lymph node DCs were not able to induce cytokine secretion in the absence of the antigenic peptide (Fig. 3 f). Thus, cytokine secretion in the DC–T cell co-culture requires the presence of specific viral antigens, and

the mere activation status of the CD4^{+} T cells, DCs, or both in combination, does not account for the cytokines observed in the co-culture.

Dendritic Cells Are the Primary APCs in IFNγ Induction from CD4^{+} T Cells. In an effort to examine the relative contribution of different APC populations in T cell priming during ivag HSV-2 infection, we isolated both the CD11c^{+} and CD11c^{−} fractions of the draining lymph node cells from mice infected ivag 5 d before. This time point was chosen based on the ability of the draining lymph node DCs between days 2 and 5 a.i. to optimally stimulate T cells in vitro as shown in Fig. 3. The CD11c-depleted population was further divided into B220^{+}/CD11c^{−} and I-A[d+]/CD11c^{−} groups (Fig. 4 a). The two populations of DCs (MHC class II[med] vs. MHC class II^{hi} cells) were present in the lymph nodes as described previously (22). When HSV-2–specific CD4^{+} T cells isolated from day 5 draining lymph nodes of HSV-2–infected mice were co-cultured with these APC populations, remarkably, only T cells stimulated with CD11c^{+} DC population secreted high levels of cytokines, whereas those stimulated with CD11c-depleted lymph node APCs or with B cells had minimal IFNγ and IL-10 secretion (Fig. 4, b and c). The lack of T cell stimulation by CD11c^{−} APCs was not due to their inherent inab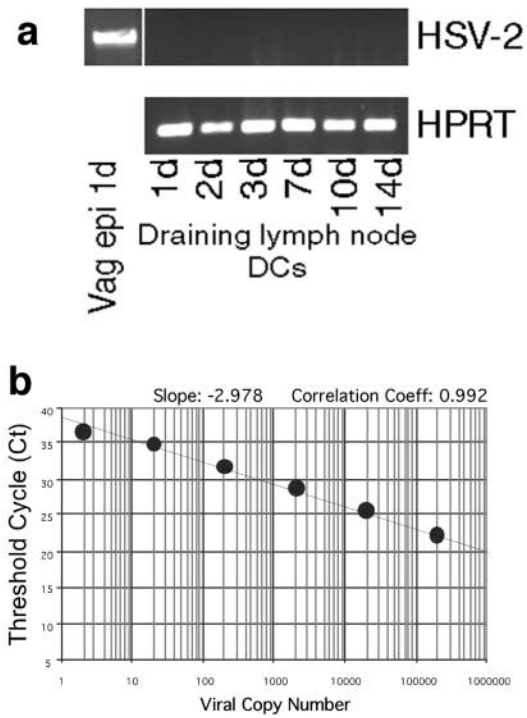ility to present antigen on MHC class II molecules because all APCs stimulated strong cytokine secretion from HSV-2–specific T cells when exogenous viral antigens were provided in vitro (Fig. 4, d and e). Together, during HSV-2 infection, CD11c^{+} DCs represent the primary APCs in stimulating IFNγ secretion from viral antigen-specific T cells in the draining lymph nodes.

Dendritic Cells Acquire HSV-2 Antigens in the Absence of Direct Infection. The draining lymph node DCs could have acquired the viral antigen either by phagocytosis of infected epithelium or by direct HSV-2 infection. To our surprise, no evidence of DC infection was detected by examination of viral protein by immunofluorescence staining (Fig. 2) or by detection of viral DNA by PCR (Fig. 5). The lower limit of detection was 30 cell-free viral particles or one infected Vero cell per reaction using our PCR protocol (Materials and Methods). To rule out the possibility of a very low number of HSV-2 viral replication within DCs, a more sensitive method of detection of viral DNA was used. 10[4] cell equivalents of total DNA from draining lymph node DCs at days 1–3 a.i. were subjected to Real-time PCR. Despite our ability to consistently detect as little as two viral DNA copies per reaction, and that approximately one million viral DNA copies were detected from vaginal epithelial layers from the same mouse, none of the DNA samples isolated from the draining lymph node DCs had demonstrable viral DNA (Fig. 5 b). Moreover, no viral DNA was detected from total lymph node cell suspension (Fig. 5 b), indicating that viral replication is strictly confined to the vaginal epithelial cells and that virus does not travel to the draining lymph nodes.

Activation of CD4^{+} T Cells in the Draining Lymph Nodes and in the Spleen. To determine the time course of T cell activation and migration in vivo, CD4^{+} T cells were isolated at various time points after ivag HSV-2 infection from the draining lymph nodes and were incubated with irradiated splenocytes from naive syngeneic mice pulsed with either heat-inactivated virus or control lysate. After a 72-h incubation in vitro, the supernatants were analyzed for secretion of IFNγ, IL-4, and IL-10 (Fig. 6). Both IFNγ and IL-10 secretions were detected from T cells within the draining lymph nodes starting at 3 d a.i. and persisted for up to 14 d a.i. Only minor levels of IL-4 were secreted from these cells. Thus, antigen-specific CD4^{+} T cells became detectable in the draining lymph nodes of ivag-infected mice at 3 d a.i. and continued to be present until 14 d. In the spleen, HSV-2–specific T cell responses were detected with a similar cytokine secretion profile to those in the draining lymph nodes. However, the appearance of HSV-2–specific T cells in the spleen began only after 5 d a.i., which represents a 2-d lag from the draining lymph node response, and disappeared by 14 d a.i. (Fig. 6).

Submucosal DCs Present Viral Peptides to CD4^{+} T Cells in the Draining Lymph Nodes. In an effort to delineate the contribution of LCs and submucosal DCs in T cell priming after HSV-2 infection, LC-derived DCs and submucosally derived DCs in the draining lymph nodes were isolated by flow cytometric cell sorting. LC-derived DCs were identified by staining with an antibody to gp40, a murine homo-


Figure 4. CD11c^{+} DCs are crucial for IFNγ secretion from HSV-2–specific T cells. Various APC populations were isolated from draining lymph nodes of day 5 infected mice by magnetic selection. CD11c^{−} fraction was obtained using the depletion column and was further subdivided into B220^{+} or I-A[d+] groups by magnetic selection. (a) A representative FACS® profile of these APC populations, gated on live cells, is shown. These APC groups were used to stimulate HSV-2–specific CD4^{+} T cells in the absence (b and c) or presence (d and e) of exogenously added heat-inactivated virus. Cytokines secreted from T cells were measured by ELISA. The data are representative of three similar experiments. Each experiment was conducted with three to four mice.

Figure 5. Draining lymph node DCs do not contain HSV-2 viral DNA. Total DNA was isolated from DCs from the draining lymph nodes of mice inoculated ivag with HSV-2 or with control cell lysate using magnetic beads. (a) HSV-2 viral DNA was amplified using specific primers by PCR. DNA isolated from 24 h HSV-2–infected vaginal epithelium was used as a positive control for HSV-2–specific gene amplification. The presence of genomic DNA in each sample is depicted by PCR amplification of the housekeeping HPRT gene. To further confirm the lack of viral DNA in the DCs and total draining lymph node cells, either 10^4 (DCs) or 10^5 (total lymph node cells) cell equivalents of DNA was subjected to Real-time PCR at days 0, 1, 2, or 3 a.i. (b). In parallel, DNA obtained from the vaginal epithelial layer (sites of viral replication) at the corresponding time points were also examined by Real-time PCR as a positive control for infection in these mice. These reactions were conducted twice with similar results.

logue of the human epithelial cell adhesion molecule (23, 24). The gp40 molecule has been previously demonstrated to be expressed specifically by LCs and not by other DCs (23, 24). The submucosal CD11c^{+} DCs were identified by the expression of CD11b because CD11b is expressed on all submucosal DCs as shown previously for dermal DCs (21). First, we confirmed that the gp40 expression was only detected in subcutaneous and vagina-draining lymph nodes and was absent in nonskin-draining lymph nodes, such as
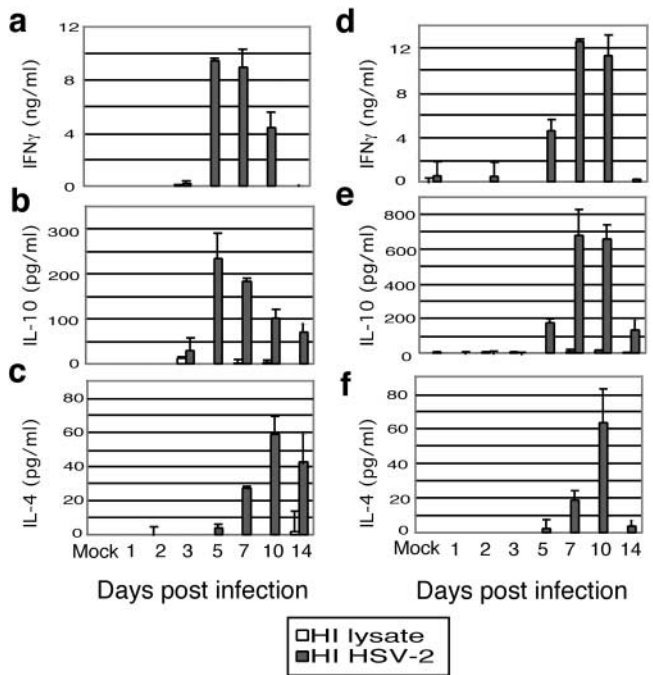
Figure 6. Cytokine secretion from CD4^{+} T cells in draining lymph nodes and spleen of ivag HSV-2–infected mice. CD4^{+} T cells positively selected from draining lymph nodes (a–c) and spleen (d–f) of mice infected ivag with 186TKΔKpn for various time periods were co-cultured with irradiated syngeneic splenocytes in the presence of heat-inactivated HSV-2 (filled bars) or heat-inactivated control cell lysate (white bars) for 3 d and supernatants were analyzed for IFNγ (a and d), IL-10 (b and e), or IL-4 (c and f).

the mesenteric lymph nodes (Fig. 7 a). Second, phenotypic analysis of the LC-derived gp40[+] DCs revealed that they were DEC205^{hi}, CD8α[lo] with moderate to high expression of CD11b (Fig. 7 b), a profile completely consistent with the phenotype of LCs in subcutaneous lymph nodes (25). The FACS® analysis of LCs (gp40^{+}) and submucosal DCs (CD11b^{+}/gp40^{−}) revealed that in the draining lymph nodes, LC population diminishes whereas submucosal DCs increase in percentage after HSV-2 infection (Fig. 7 b). Strikingly, when the antigen-presenting capacity of these DC populations were compared, only the CD11b^{+} submucosal DCs, but not gp40^{+} LCs, were found to present viral antigens to CD4^{+} T cells (Fig. 7 c), despite their equal ability to present exogenously added viral antigens to HSV-2–specific CD4^{+} T cells (Fig. 7 d). Next, the ability of the other major lymph node DC subset, namely the CD8α^{+} DCs, to present viral antigens to CD4^{+} T cells was examined. The CD8α^{+} DCs have been shown to play a critical role in cross-presentation of cell-associated antigens (26–28). FACS® analysis of CD8α^{+} DCs revealed that they also do not present HSV antigens to CD4^{+} T cells in the draining lymph nodes (Fig. 7, c and d). Together, these data collectively show that submucosal DCs are recruited to the infected epithelium, phagocytose exogenous viral antigens, migrate to the draining lymph nodes, and are uniquely capable of presenting viral antigenic peptides to CD4^{+} T cells.
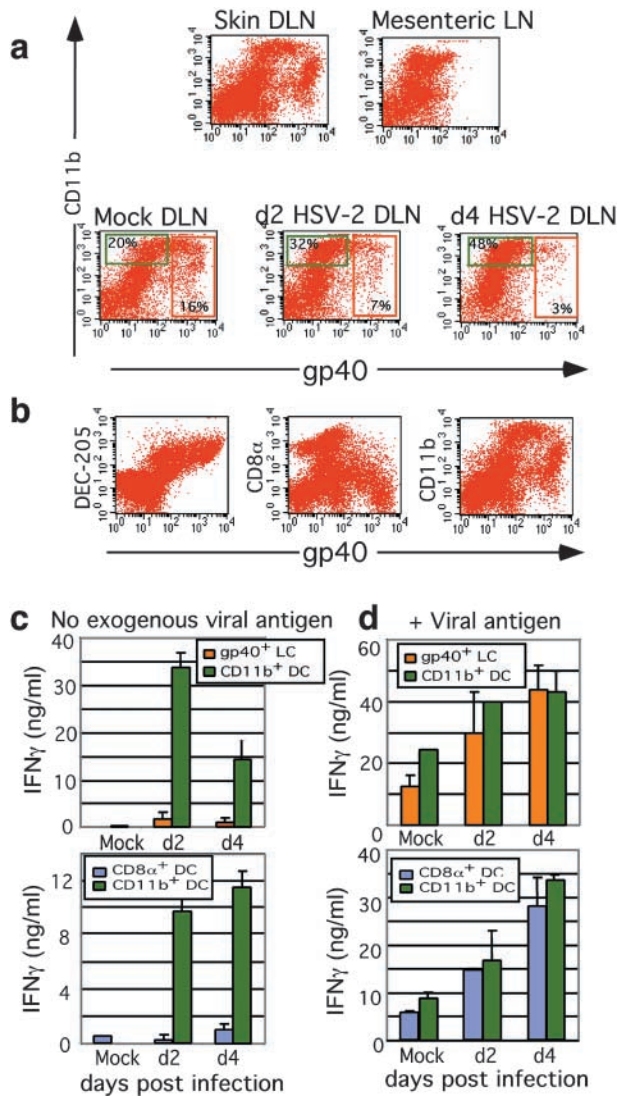
Figure 7. Submucosal DCs, but not Langerhans cells or CD8α^{+} DCs, present viral peptides to CD4^{+} T cells in the draining lymph nodes. To differentiate the contribution of LCs and submucosal DCs in the presentation of HSV-2 antigens in vivo, CD11c^{+} cells were stained with gp40 (LC) and CD11b (submucosal DC) after HSV-2 ivag infection at 2 or 4 d a.i. and were analyzed by flow cytometry (a). The DC markers, DEC-205, CD8α, and CD11b, on CD11c^{+} cells were analyzed (b). The LC-derived (gp40^{+}), submucosal DCs (CD11b^{+}), or the CD8α^{+} DCs were FACS®-sorted from draining lymph nodes at 2 or 4 d a.i. and were co-cultured with HSV-2–specific CD4^{+} T cells in the absence (c) or presence (d) of viral antigens for 72 h. IFNγ secreted from T cells were analyzed by ELISA (c and d).

Discussion

The mechanism of immune induction to ivag HSV-2 infection is unclear. To better understand the contribution of the vaginal APCs in immune induction to HSV-2, we first examined the distribution of LCs and submucosal DCs in the uninfected vaginal tissues at different stages of the estrous cycle. We demonstrate here that LCs are present during estrous and metestrous-1 only near the base of the epithelium. Because cornified epithelium covers the vaginal mucosa during these stages of the estrous cycle, access by

infectious agents to deeper tissues is likely limited. Evolutionarily, the localization of LCs near the mucosal surface may not have been necessary during these particular stages of the menstrual cycle when such a physical protective barrier is provided. On the other hand, during the metestrous-2 and diestrous phases when the shedding of this barrier occurs, the opportunity for sexually transmitted pathogens to invade the host is greatly enhanced due to the lack of protective cornified epithelium and the reduced thickness of the stratum spinosum. Consequently, a higher number of LCs may have been necessary to survey invading microbes at these stages. In the case of HSV-2 infection, mice are found to be susceptible to viral infection only during these catabolic stages (3–6).

The current paradigm of immune induction to infectious agents at body surfaces covered by squamous epithelium such as the skin and the vagina is that LCs encounter pathogens within the epithelium, take up antigens from the pathogens, and migrate to the draining lymph nodes to prime naive T cells (29). In our current work, the rampant HSV-2 infection of the vaginal epithelium resulted in the complete lysis of the cells in this layer, destroying LCs in this tissue within 48 h a.i. However, rapid recruitment of submucosal CD11c^{+} DCs just beneath the infected epithelium was observed within 24 h a.i., followed by a subsequent appearance of CD11c^{+}/CD11b^{+} DCs presenting the viral peptides in the draining lymph nodes by 48 h a.i. To decipher the relative roles of LCs and submucosal DCs in antigen presentation and T cell activation in the draining lymph nodes, LCs and submucosal DCs were isolated by FACS® from draining lymph nodes after HSV-2 infection. Stimulation of HSV-2–specific T cells revealed that only the submucosal DCs, and not LCs, presented viral antigens to CD4^{+} T cells (Fig. 7). Our observations that submucosal DCs, but not LCs, are the primary cells responsible for T cell priming in the draining lymph nodes after ivag HSV-2 infection are also supported in a paper by Parr et al., which tracked the emigrant cells from vaginal epithelium with a fluorescent dye (12). With this method, no migration of the LCs from the vaginal epithelium to the draining iliac lymph nodes was observed after ivag HSV-2 infection (12). Furthermore, we examined the antigen-presenting capacity of the CD8α[+] lymph node DCs that have been shown to be responsible for presenting cell-associated antigens to T cells in vivo (26–28). Comparison of the ability of the two major subsets of DCs in the draining lymph nodes clearly demonstrates that only the CD11b^{+} DCs, but not CD8α^{+} DCs, present in vivo–derived viral peptides to CD4^{+} T cells (Fig. 7, c and d). These results indicate that the viral antigens are presented directly by the CD11b^{+} DCs in the absence of either antigen transfer to the lymph node CD8α^{+} DC or the differentiation of these cells to the CD8α^{+} phenotype. Together, our data demonstrate a previously unrevealed role of the submucosal DCs in antigen presentation to CD4^{+} T cell after ivag HSV-2 infection, and further provide evidence for the lack of participation by LCs and the CD8α^{+} DCs in this process.

Several studies have examined the consequences of direct infection of DCs by HSV-1 in vitro. Human DCs have been shown to express some of the receptors required to mediate the entry of HSV such as Hve-A and Hve-B and can be infected by HSV-1 in vitro (30, 31). HSV-1 infection was shown to inhibit maturation of immature DCs (30, 31) and their ability to prime naive T cells (31). Our in vivo examination with TK⁻ HSV-2 revealed that the infection was not detected within the emigrant DC populations in the draining lymph nodes, despite the proximity of recruited submucosal DCs to the infected epithelium. In fact, the draining lymph nodes did not contain any viral DNA. Our finding is consistent with the paper by Mueller et al., which demonstrates that despite rapid activation of CD8⁺ T cells after footpad HSV-1 infection, the draining lymph nodes contained no viral DNA (32). The difference in the infectivity of human blood DCs to HSV-1 in vitro and mouse genital submucosal DCs to HSV-2 in vivo may be explained by a number of factors, including the difference in expression of Hves (unpublished data) and the fact that murine Hve-B does not function as a viral entry mediator for HSV (33). Productive replication of HSV-2 was strictly confined to the epithelial layer, within which LCs reside. Thus, our data suggest that LCs may be inhibited from performing antigen-presenting functions as a result of the lytic destruction of the epithelial layer. This hypothesis is supported by the progressive reduction of the number of LCs in draining lymph nodes after HSV-2 infection (Fig. 7 a). Conversely, we show that HSV-2 infection of the epithelium did not lead to suppression, but instead to activation of the phenotype and function of the neighboring uninfected submucosal DCs. The factors released by the HSV-infected epithelial cells, or the virus itself, are likely responsible for inducing activation of the submucosal DCs.

A clear picture of immune inductive events after ivag HSV-2 infection emerges from our work. Upon entry into vaginal lumen, HSV-2 specifically infects the diestrous vaginal epithelium. This infection event results in the recruitment of submucosal DCs toward the infected epithelium, presumably from both local lamina propria and peripheral sources. After recruitment, the foci of DCs directly beneath the infected epithelium form within 24 h and DCs continue to accumulate for several days. This event in the vaginal mucosa is accompanied by the appearance of DCs that harbor HSV-2 peptide on their cell surface MHC class II capable of stimulating HSV-2–specific T cells in the draining lymph nodes. The DCs that migrate to the draining lymph nodes during the first 2–3 d a.i. express higher levels of costimulatory molecules, and are thus capable of stimulating antigen-specific T cells. Lagging 1 d behind, CD4⁺ T cells capable of secreting high levels of IFNγ and moderate levels of IL-10 in an HSV-2–specific manner begin to become detectable in the draining lymph nodes first, and subsequently in the spleen. The HSV-2–specific Th1 cells found in the spleen likely migrated from the priming lymph nodes because we detected no evidence of antigen-presenting DCs in the spleen or in any other nondraining lymph nodes at any time points examined. To our surprise, despite the fact that numerous CD4⁺ T cells were present in the draining lymph nodes at 14 d a.i., we did not detect cytokine secretion from CD4⁺ T cells by this time point. Furthermore, HSV-2–specific CD4⁺ T cells were not found in the spleen at this time. It is possible that regulatory T cells develop in these tissues that prohibit secretion of cytokines from effector Th1 cells. Alternatively, the HSV-2–specific effector memory T cells may have migrated to nonlymphoid tissues as described for lymphocytic choriomeningitis virus (34). In support of the latter possibility, despite our inability to detect effector T cells in the lymphoid tissues after 14 d a.i., these cells are clearly present and are recruited rapidly to the sites of infection and mediate protective immunity during secondary viral challenges (8, 9).

Our data provide the first evidence of the critical role played by the submucosal vaginal DCs in eliciting IFNγ-mediated CD4⁺ T cell responses during ivag HSV-2 infection. Because the expression of receptors and adhesion molecules for various sexually transmitted pathogens may differ significantly between the submucosal DCs and LCs of the vaginal mucosa (35), our results suggest the importance of the involvement of the submucosal vaginal DC populations in disease pathogenesis and in immune induction to other microbial agents of sexually transmitted diseases.

References

1. Lenz, A., M. Heine, G. Schuler, and N. Romani. 1993. Human and murine dermis contain dendritic cells. Isolation by means of a novel method and phenotypical and functional characterization. *J. Clin. Invest.* 92:2587–2596.
2. Meunier, L., A. Gonzalez-Ramos, and K.D. Cooper. 1993. Heterogeneous populations of class II MHC+ cells in human dermal cell suspensions. Identification of a small subset responsible for potent dermal antigen-presenting cell activity with features analogous to Langerhans cells. *J. Immunol.* 151: 4067–4080.
3. Baker, D.A., and S.A. Plotkin. 1978. Enhancement of vaginal infection in mice by herpes simplex virus type II with progesterone. *Proc. Soc. Exp. Biol. Med.* 158:131–134.
4. Gallichan, W.S., and K.L. Rosenthal. 1996. Effects of the estrous cycle on local humoral immune responses and protection of intranasally immunized female mice against herpes simplex virus type 2 infection in the genital tract. *Virology.* 224:487–497.
5. Overall, J.C., Jr., E.R. Kern, R.L. Schlitzer, S.B. Friedman, and L.A. Glasgow. 1975. Genital herpesvirus hominis infection in mice. I. Development of an experimental model. *Infect. Immun.* 11:476–480.
6. Parr, M.B., L. Kepple, M.R. McDermott, M.D. Drew, J.J.

Bozzola, and E.L. Parr. 1994. A mouse model for studies of mucosal immunity to vaginal infection by herpes simplex virus type 2. *Lab. Invest.* 70:369–380.

7. McDermott, M.R., J.R. Smiley, P. Leslie, J. Brais, H.E. Rudzroga, and J. Bienenstock. 1984. Immunity in the female genital tract after intravaginal vaccination of mice with an attenuated strain of herpes simplex virus type 2. *J. Virol.* 51:747–753.

8. Harandi, A.M., B. Svennerholm, J. Holmgren, and K. Eriksson. 2001. Differential roles of B cells and IFN-gamma-secreting CD4(+) T cells in innate and adaptive immune control of genital herpes simplex virus type 2 infection in mice. *J. Gen. Virol.* 82:845–853.

9. Parr, M.B., and E.L. Parr. 1999. The role of gamma interferon in immune resistance to vaginal infection by herpes simplex virus type 2 in mice. *Virology.* 258:282–294.

10. McDermott, M.R., L.J. Brais, and M.J. Evelegh. 1990. Mucosal and systemic antiviral antibodies in mice inoculated intravaginally with herpes simplex virus type 2. *J. Gen. Virol.* 71:1497–1504.

11. Parr, M.B., and E.L. Parr. 1997. Protective immunity against HSV-2 in the mouse vagina. *J. Reprod. Immunol.* 36:77–92.

12. King, N.J., E.L. Parr, and M.B. Parr. 1998. Migration of lymphoid cells from vaginal epithelium to iliac lymph nodes in relation to vaginal infection by herpes simplex virus type 2. *J. Immunol.* 160:1173–1180.

13. Jones, C.A., T.J. Taylor, and D.M. Knipe. 2000. Biological properties of herpes simplex virus 2 replication-defective mutant strains in a murine nasal infection model. *Virology.* 278:137–150.

14. Gao, M., and D.M. Knipe. 1989. Genetic evidence for multiple nuclear functions of the herpes simplex virus ICP8 DNA-binding protein. *J. Virol.* 63:5258–5267.

15. Green, E.L. 1989. Biology of the Laboratory Mouse. 2nd ed. Dover Publications, New York. 716 pp.

16. Green, E.L. 1966. Biology of the Laboratory Mouse, by the Staff of the Jackson Laboratory. 2nd ed. Dover Publications, New York. 706 pp.

17. Iwasaki, A., and B.L. Kelsall. 2001. Unique functions of CD11b+, CD8 alpha+, and double-negative Peyer's patch dendritic cells. *J. Immunol.* 166:4884–4890.

18. Iwasaki, A., and B.L. Kelsall. 1999. Freshly isolated Peyer's patch, but not spleen, dendritic cells produce interleukin 10 and induce the differentiation of T helper type 2 cells. *J. Exp. Med.* 190:229–239.

19. Kelsall, B.L., and W. Strober. 1996. Distinct populations of dendritic cells are present in the subepithelial dome and T cell regions of the murine Peyer's patch. *J. Exp. Med.* 183:237–247.

20. Hobson, A., A. Wald, N. Wright, and L. Corey. 1997. Evaluation of a quantitative competitive PCR assay for measuring herpes simplex virus DNA content in genital tract secretions. *J. Clin. Microbiol.* 35:548–552.

21. Anjuere, F., P. Martin, I. Ferrero, M.L. Fraga, G.M. del Hoyo, N. Wright, and C. Ardavin. 1999. Definition of dendritic cell subpopulations present in the spleen, Peyer's patches, lymph nodes, and skin of the mouse. *Blood.* 93:590–598.

22. Salomon, B., J.L. Cohen, C. Masurier, and D. Klatzmann. 1998. Three populations of mouse lymph node dendritic cells with different origins and dynamics. *J. Immunol.* 160:708–717.

23. Borkowski, T.A., J.J. Letterio, A.G. Farr, and M.C. Udey. 1996. A role for endogenous transforming growth factor β1 in Langerhans cell biology: the skin of transforming growth factor β1 null mice is devoid of epidermal Langerhans cells. *J. Exp. Med.* 184:2417–2422.

24. Borkowski, T.A., A.J. Nelson, A.G. Farr, and M.C. Udey. 1996. Expression of gp40, the murine homologue of human epithelial cell adhesion molecule (Ep-CAM), by murine dendritic cells. *Eur. J. Immunol.* 26:110–114.

25. Henri, S., D. Vremec, A. Kamath, J. Waithman, S. Williams, C. Benoist, K. Burnham, S. Saeland, E. Handman, and K. Shortman. 2001. The dendritic cell populations of mouse lymph nodes. *J. Immunol.* 167:741–748.

26. den Haan, J.M., S.M. Lehar, and M.J. Bevan. 2000. CD8(+) but not CD8(−) dendritic cells cross-prime cytotoxic T cells in vivo. *J. Exp. Med.* 192:1685–1696.

27. Iyoda, T., S. Shimoyama, K. Liu, Y. Omatsu, Y. Akiyama, Y. Maeda, K. Takahara, R.M. Steinman, and K. Inaba. 2002. The CD8+ dendritic cell subset selectively endocytoses dying cells in culture and in vivo. *J. Exp. Med.* 195:1289–1302.

28. Pooley, J.L., W.R. Heath, and K. Shortman. 2001. Cutting edge: intravenous soluble antigen is presented to CD4 T cells by CD8− dendritic cells, but cross-presented to CD8 T cells by CD8+ dendritic cells. *J. Immunol.* 166:5327–5330.

29. Janeway, C.A., P. Travers, M. Walport, and M. Shlomchik. 2001. Immunobiology. 5th ed. Garland Publishing, New York. 732 pp.

30. Mikloska, Z., L. Bosnjak, and A.L. Cunningham. 2001. Immature monocyte-derived dendritic cells are productively infected with herpes simplex virus type 1. *J. Virol.* 75:5958–5964.

31. Salio, M., M. Cella, M. Suter, and A. Lanzavecchia. 1999. Inhibition of dendritic cell maturation by herpes simplex virus. *Eur. J. Immunol.* 29:3245–3253.

32. Mueller, S.N., C.M. Jones, C.M. Smith, W.R. Heath, and F.R. Carbone. 2002. Rapid cytotoxic T lymphocyte activation occurs in the draining lymph nodes after cutaneous herpes simplex virus infection as a result of early antigen presentation and not the presence of virus. *J. Exp. Med.* 195:651–656.

33. Shukla, D., C.L. Rowe, Y. Dong, V.R. Racaniello, and P.G. Spear. 1999. The murine homolog (Mph) of human herpesvirus entry protein B (HveB) mediates entry of pseudorabies virus but not herpes simplex virus types 1 and 2. *J. Virol.* 73:4493–4497.

34. Masopust, D., V. Vezys, A.L. Marzo, and L. Lefrancois. 2001. Preferential localization of effector memory cells in nonlymphoid tissue. *Science.* 291:2413–2417.

35. Jameson, B., F. Baribaud, S. Pöhlmann, D. Ghavimi, F. Mortari, R.W. Doms, and A. Iwasaki. 2002. Expression of DC-SIGN by intestinal and genital mucosal dendritic cells in humans and rhesus macaques. *J. Virol.* 76:1866–1875.